

Automatic Cobb Angle Measurement System by Using Nuclear Medicine Whole Body Bone Scan

Jia-Yann Huang
Department of Electrical Engineering,
Yuan Ze University,
Chungli, Taiwan, ROC
john@adm.cgmh.org.tw

Pan-Fu Kao
Department of Nuclear Medicine,
Buddhist Tzu Chi General
Hospital, Taipei, Taiwan, ROC
kaopanfu@tzuchi.com.tw

Yung-Sheng Chen
Department of Electrical Engineering,
Yuan Ze University,
Chungli, Taiwan, ROC
eeyschen@saturn.yzu.edu.tw

Abstract

Evaluation of scoliosis is performed traditionally by means of standing posterior-anterior radiographs of the full spine to assess lateral curvature with the Cobb method. In this paper, we present a new automatic algorithm to measure Cobb angle by using nuclear medicine whole body bone scan images. Our algorithm design is based on the fuzzy sets histogram thresholding, anatomical knowledge-based image segmentation method, and morphology technology. It is expected that the results may help physicians to diagnose scoliosis via the scintigraphy images, and thus to reduce radiation done to patients.

1 Introduction

Scoliosis is defined as the lateral deviation of spinal curve in the coronal plane. The Cobb angle has become the basis for quantifying scoliosis curve magnitude [1-2]. The most tilted vertebral bodies above and below the apex of the spinal curve are used to create intersecting lines that produce the curve degree as shown in Figure 1. This definition is controversial, and patients do not exhibit clinically significant respiratory symptoms with idiopathic scoliosis until their curves become 60 to 100 degrees. Radiographic examination is the imaging modality that is generally employed to describe spine curves by their appearance on plain films and quantified by the magnitude of the Cobb angle derived from the radiograph.

In order to reduce the risk of breast cancer caused by multiple diagnostic x-rays during childhood and adolescence [3], many non-invasive Cobb angle measurement methods were developed [4]. The main non-invasive technologies include the uses of the Scoliometer (SCOL), back-contour device (BCD), and moiré topographic imaging (MTI). Amend et al [5] showed that the SCOL method has a good reproducibility, but the correlation for the measurement of lateral curvature was low. The back surface characteristics are similar to the use of BCDs [6-9]. The BCD consists of a level frame through which passes a series of movable rods. These rods may be locked in position to record the contour of the opposing back surface of the patient in the forward-bending position. A complete surface contour of a subject's back can be reproduced from an MTI [10-11], but this is a complex procedure requiring much expertise.

Stocks et al [12-13] adopted a computer-aided diagnosis (CAD) algorithm to minimize human involvement in Cobb angle measurement and, in King et al classification, identify potential sources of classification errors. They marked four points on each vertebral body and, two points

on the sacrum, as determined from the landmarks by the computerized algorithm, the curve pattern was automatically classified.

Our motivation of this study is to evaluate scoliosis by nuclear medicine whole body bone scan. Most patients with scoliosis will perform bone scan to exclude any focal bony abnormalities [14]. At the same time, we can measure the Cobb angle automatically by our algorithm to measure lateral curvature, which may potentially prevent patients from receiving additional routine x-ray exposures.

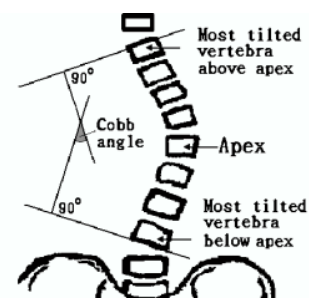


Figure 1. Illustration of the Cobb angle measurement by Cobb method.

2 Method and materials

Our algorithm contains preprocessing, image segmentation, and automatic Cobb angle measurement. The first step includes a) removing the noise outside the body region; b) applying Gaussian smoothing to compress the influence of noise inside the body region; and c) adopting histogram equalization method to enhance the image quality. The second step is to segment the back region including vertebrae and ribs from the whole body bone scan. The third step is the automatic Cobb angle measurement.

The images of nuclear medicine whole body bone scan in anterior view and posterior view were obtained by a dual-head gamma camera [15]. Figure 2a shows the posterior view of a whole body bone scan.

2.1 Preprocessing

The noise outside the body region were clearly demonstrated on an over adjusted bright image (Figure 2a). The histogram of the image revealed a deep valley between two peaks at the low gray level area (Figure 2b). A threshold value at valley of the histogram was applied to eliminate noise. The noise inside the body region was removed by applying an isotropic Gaussian filter with a

standard derivation of 1.4. Finally, a histogram equalization method was applied to improve the image quality by the following equation:

$$f(I_A) = G_{\max} \int_0^{I_A} p_A(u) du. \quad (1)$$

I_A is the input image, G_{\max} is denoted as the maximum value in the gray-level scale, and $p_A(u)$ is the probability mass function of input image.

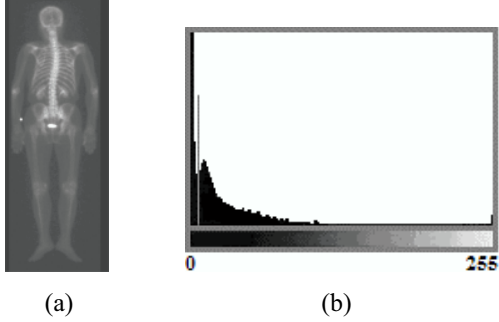


Figure 2. (a) The posterior view of a whole body bone image with noises outside the body frame. (b) The histogram of a whole body bone in posterior view.

2.2 Image segmentation

The purpose of image segmentation was to segment the back region which includes vertebrae and ribs apart from the posterior whole body bone scan. It will facilitate the processing in the automatic Cobb angle measurement procedure.

2.2.1 Fuzzy sets histogram thresholding

To locate the typical reference points in skeleton, the pixels of soft tissue should be compressed and those of bone around typical reference points be reserved. By using fuzzy sets on histogram thresholding, Tobias and Seara demonstrated successfully in separation background from object in multimodal and bimodal histogram images [16]. We applied this algorithm to classify soft tissue and bone regions. This algorithm can be summarized as follows.

The fuzzy set A is characterized by the function $\mu_A = (x_i)$, the S -function is used for modeling the membership function. This function is defined as below:

$$\mu_{A-S}(x) = S(x, a, b, c) = \begin{cases} 0, & x \leq a \\ 2((x-a)/(c-a))^2, & a < x \leq b \\ 1 - 2((x-c)/(c-a))^2, & b < x \leq c \\ 1, & x > c. \end{cases} \quad (2)$$

The parameter b denotes the crossover point, which is given by $b = (a+c)/2$, with $\mu_{A-S} = 0.5$; the bandwidth is defined as $\Delta b = b - a = c - b$. The Z -function, which is derived from the S -function as below:

$$\mu_{A-Z}(x) = Z(x, a, b, c) = 1 - S(x, a, b, c). \quad (3)$$

By using the IF introduced by Kaufman [17], we can determine how compact the set it is as compared with its nearest ordinary set, and is given as:

$$\mu_{\bar{A}}(x_i) = \begin{cases} 0, & \text{if } \mu_A(x_i) < 0.5 \\ 1, & \text{if } \mu_A(x_i) \geq 0.5. \end{cases} \quad (4)$$

This index is obtained by measuring the distance between A and \bar{A} , and is defined as:

$$\psi_k = \frac{2}{n^{1/k}} d_k(A, \bar{A}). \quad (5)$$

The $d_k(A, \bar{A})$ is a measurement of distance, and n is the number of elements in \bar{A} . Such a distance calculation can be simplified as follows:

$$\begin{aligned} d_k(A, \bar{A}) &= \frac{2}{n} \sum_{i=1}^n |\mu_A(x_i) - \mu_{\bar{A}}(x_i)| \\ &= \frac{2}{n} \sum_{i=1}^n \min(\mu_A(x_i), 1 - \mu_A(x_i)) \\ &= \frac{2}{n} \sum_{k=0}^{255} (\min(\mu_A(k), 1 - \mu_A(k))) \times h(k). \end{aligned} \quad (6)$$

Two linguistic variables {soft tissue, bone} modeled by two fuzzy subsets of U , denoted by S and B , respectively. The fuzzy subsets S and B are associated with the histogram intervals $[x_{\min}, x_j]$ and $[x_r, x_{\max}]$, respectively, where x_j and x_r are the final and initial gray level limits for these subsets; the x_{\min} and x_{\max} are the lowest and highest gray levels of the image, respectively. The gray levels in each of these subsets have the intuitive property of belonging with certainty to the final subsets object (O) or background (F). That is, $S \subset F$ and $B \subset O$. With these subsets, a seed for starting the similarity measure process was obtained. To obtain the segmented version of the gray level image, each gray level of the fuzzy region has to be classified as object (bone) or background (soft tissue). For classification procedure, a gray level picked from the fuzzy region was added to each of the seed subsets. By measuring the IF's of the subsets $S \cup \{x_i\}$ and $B \cup \{x_i\}$, the x_i was assigned to the subset with lower IF with the maximum similarity. By applying this procedure for all gray levels of the fuzzy region (Figure 3), each pixel was classified into object or background subsets. The proposed classification method performs the comparison of IF measures, we need to normalize those measures. This is archived by first computing the IF's of the seed subsets S and B , and by computing a normalization factor α according to the following relation:

$$\alpha = \psi_k(S) / \psi_k(B). \quad (7)$$

Where $\psi_k(S)$ and $\psi_k(B)$ are the IF's of the subsets S and B , respectively. Figure 3 shows how the normalization works. The thresholding result of scintigraphy in posterior view was illustrated in Fig 4a, and was denoted as I_{PA}^{fuzzy} .

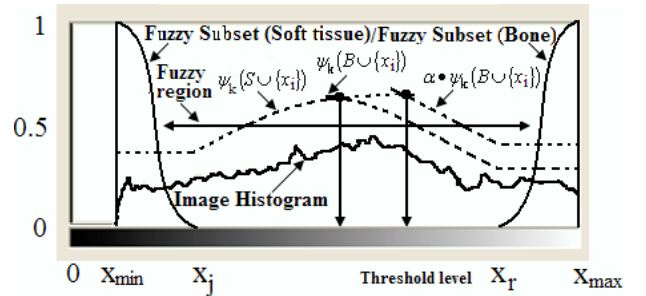


Figure 3. Illustrations of image histogram, characteristic functions for the seed subsets, normalization step (dotted lines) of the indices of fuzziness, and determination of the threshold value.

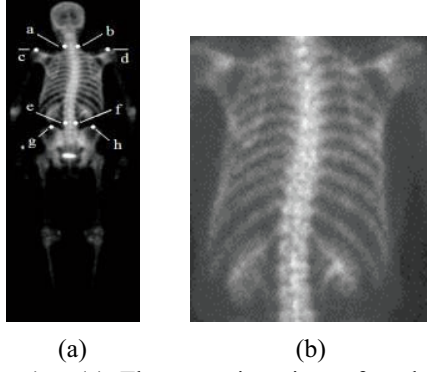


Figure 4. (a) The posterior view of a thresholded whole body bone image with reference points. (b) The segmented region including vertebrae and ribs.

2.2.2 Locate reference points

After performing the fuzzy sets histogram thresholding, the I_{PA}^{fuzzy} image was adopted to locate neck, shoulder, vertebra, and pelvis reference points by anatomical knowledge [18].

From top to 25% height of the image in vertical direction, the image width formed by the most left and right margin was calculated in each row, the most left and right margins with minimum image width were defined as P^{Neck-L} and P^{Neck-R} for neck reference points, labeled as 'a', 'b' in Figure 4a respectively.

From P^{Neck-L} to 25% image height in vertical direction, the horizontal distances from left image extremity to the first pixel with a non-zero gray level were calculated for each row. Once the distance difference was greater three times than previous one, then the left apex of shoulder was located and was denoted as $P^{Shoulder-L}$ (labeled as 'c' in Figure 4a). The similar way was applied to locate the right apex of shoulder, and was denoted as $P^{Shoulder-R}$ (labeled as 'd' in Figure 4a)

Beginning from 30% to 50% image height in vertical direction, we determined the minimum width which was formed by the most left and right margins in a row, and marked the coordinates of margins to derive the vertebra reference points which were denoted as P^{Ver-L} and P^{Ver-R} (labeled as 'e', 'f' in Figure 4a respectively).

Downward from P^{Ver-L} , the horizontal distances between the horizontal coordinate of $P^{Shoulder-L}$ and the left-first non-zero gray level pixel was detected in every row. If the distance difference exceeded three times than previous one, then the left-top of pelvis was located. The right-top of pelvis was located with the similar way. We denoted the left-top reference point as $P^{Pelvis-L}$ (labeled as 'g' in Figure 4a), and right-top reference point as $P^{Pelvis-R}$ (labeled as 'h' in Figure 4a).

3 Automatic Cobb angle measurement

As shown in Figure 4b, the region including vertebra and ribs was segmented apart from the whole body scan by the reference points of $P^{Shoulder-L}$, $P^{Shoulder-R}$, $P^{Pelvis-L}$, and $P^{Pelvis-R}$, then histogram thresholding using fuzzy sets as mentioned in 2.2.1 was applied in the segmented region again. Following, the image was converted from a gray level image into a binary image (Figure 5a). Figure 5b demonstrates the reverse image of Figure 5a.

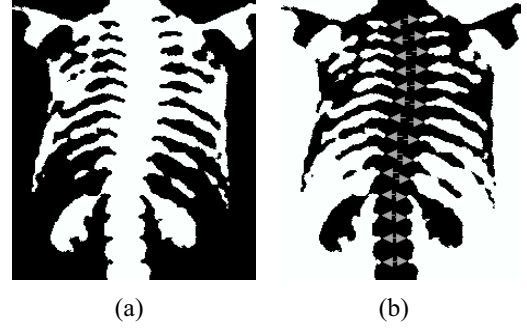


Figure 5. (a) Illustration of the segmented binary image. (b) The reverse binary image of (a), the margins of intervertebrae discs were pointed by arrow-type marks.

Cobb angle is the angle subtended between lines drawn along the upper border of the most tilted vertebrae above the curve's apex and the lower border of the most tilted vertebrae below the apex. Because the low-resolution characteristic of nuclear medicine whole body bone scan, it is hard to find the slant angle of each vertebrae body by itself. In another way, as shown in Figure 5b, the margins (pointed by arrow-type marks) of intervertebral discs in both sides were with a clear presentation. Hence we can adopt the two margins of every intervertebral disc to obtain its slant angle.

The exact positions of intervertebral disc margins can be obtained by applying an image thinning algorithm [19], which can be summarized as follows. The thinning of a set A by a structuring elements set $\{B\}$, denoted $A \otimes \{B\}$, can be defined in terms of the hit-or-miss transform:

$$A \otimes \{B\} = \left(\left(\dots \left((A \otimes B^1) \otimes B^2 \right) \dots \right) \otimes B^n \right) \quad (8)$$

Figure 6 demonstrates a set of structuring elements commonly used for thinning method.

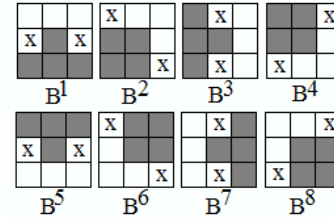


Figure 6. Illustration of the eight sequential structuring elements used by thinning algorithm.

After performing thinning processes in Figure 5a and Figure 5b, the results were shown in Figure 7a and Figure 7b, separately. We combined the segmented region (Figure 4b), the vertebrae trace (Figure 7a), and thinning image (Figure 7b) to a single image frame (Figure 7c), and it was found that the positions of intervertebral margins coincide with the anatomical structure significantly.

As shown in Figure 7d, along the vertebrae trace, we connected the two symmetrical margins of every intervertebral disc to form a line for slant angle measurement. The slant angles of the most tilted vertebrae above the curve's apex and the most tilted vertebrae below the apex were obtained, and denoted as Ang_a and Ang_b , separately.

Finally, Cobb angle can be found by the following equation:

$$Cobb\ angle = Ang_a + Ang_b. \quad (9)$$

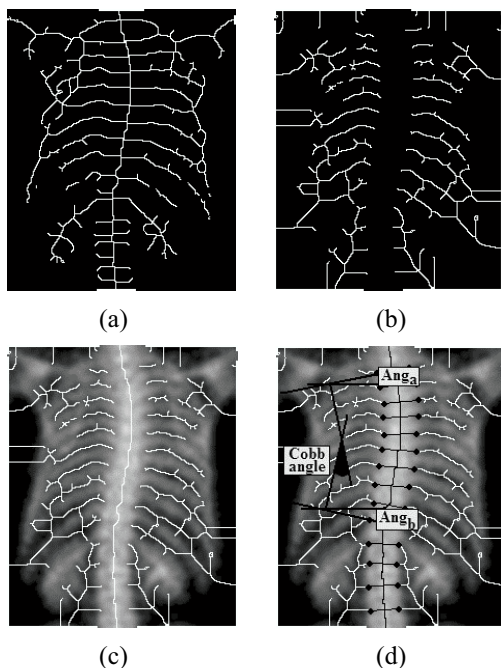


Figure 7. (a) The thinning image transferred from Figure 5a. (b) The thinning image transferred from Figure 5b. (c) The combined image of the back region, vertebrae trace, and Figure 7b. (d) The process of Cobb angle measurement.

4 Results and conclusion

In order to evaluate the proposed algorithm in this paper, we implemented a program constructed by C++ Builder 6.0, and performed experiments on an image database from the department of nuclear medicine, Buddhist Tzu Chi General Hospital at Taipei. At 3 hours after intravenous injection of $^{99m}\text{Tc-MPD}$, the whole body bone scan images were acquired by a dual-head gamma camera (GE, infinia, USA).

There were 11 random selected whole body scan images for testing, and were compared with the results obtained manually by an experienced physician (Figure 8), the mean difference was 4.14 degrees.

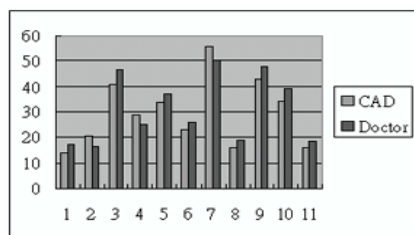


Figure 8. The comparison of our experiment results with an experienced physician's measurements.

From the experiments, our algorithm performed with an acceptable result, it is possible to be applied in clinical application practically.

Up to now, CAD applications in the field of nuclear medicine whole body bone scan are still quite few. Based on the proposed approach, for the benefits of patients, it is expected to encourage developments of other new clinical applications in nuclear medicine field.

References

- [1] C. JR: "Outline for the study of scoliosis," *Am Acad Surg Lect*, vol.5, pp.261-275, 1948.
- [2] H.L. Keim: "Scoliosis," *Clin Symp*, vol.30, pp.4-20, 1978.
- [3] M.M. Doody, J.E. Lonsteinn, M. Stovall, D.G. Luckyanov, and C.E. Land: "Breast cancer mortality after diagnostic radiography," *U.S. Scoliosis Cohort Study. Spine*, vol.25, pp.2052-2063, 2000
- [4] D.J. Pearsall, J.G. Reid, and D.M. Hedden: "Comparison of three noninvasive methods for measuring scoliosis," *Physical Therapy*, vol.72, no. 9, pp.648-657, 1992.
- [5] L.E. Amendt, K.L. Ellias, J.L. Eybers, et al: "Validity and reliability testing of the Scoliometer," *Physical Therapy*, vol. 70, pp.108-117, 1990.
- [6] E.J. Rogala, D.S. Drummond, and J. Gurr: "Scoliosis incidence and natural history: a prospective epidemiological study," *J Bone Joint Surg AM*, vol.60, pp.173-176, 1978.
- [7] R.G. Burwell, N.J. James, F. Johnson, et al: "The rib hump score: a guide to referral and prognosis," *J Bone Joint Surg Br*, vol.64, pp.284, 1982.
- [8] R.G. Burwell, N.J. James, F. Johnson, et al: "Standardized trunk asymmetry scores: a study of back contour in healthy school children," *J Bone Joint Surg Br*, vol. 65, pp.452-463, 1983.
- [9] T. Thulbourne and R. Gillespie: "The rib hump in idiopathic scoliosis: measurement, analysis, and response to treatment," *J Bone Joint Surg Br*, vol.58, pp.64-71, 1976.
- [10] M. Batouche, R. Benlamri, and M.K. Kholadi: "A computer vision system for diagnosing scoliosis using moiré images," *Comput Biol Med*, vol.26, no.4, pp.339-353, 1996.
- [11] A.M. Years, R.G. Pena, and R. Junco: "Moire topography: alternative technique in health care," *Optics and Lasers in Engineering*, vol.40, no.1, pp.105-116, 2003.
- [12] I.A. Stokes and D.D. Aronsson: "Identifying sources of variability in scoliosis classification using a rule-based automated algorithm," *Spine*, vol.27, pp.2801-2805, 2002.
- [13] I.A. Stokes and D.D. Aronsson: "Computer-Assisted algorithms improve reliability of King classification and Cobb angle measurement of scoliosis," *Spine*, vol.31, pp.665-670, 2006.
- [14] N. Wright: "Imaging in scoliosis," *Arch. Dis Child*, vol.82, pp.38-40, 2000.
- [15] A. Ho: "Scintillation camera with multichannel collimators," *J Nucl Med*, vol.5, pp.515-531, 1964.
- [16] O.J. Tobias and R. Seara: "Image segmentation by histogram thresholding using fuzzy sets," *IEEE Transactions on Image Processing*, vol.11, pp.1457-1465, 2002.
- [17] A. Kaufmann: *Introduction to the Theory of Fuzzy Subsets*, Academic Press, New York, 1975.
- [18] E.N. Marieb and J. Mallatt: *Human Anatomy*, Addison Wesley, Longman, 1998.
- [19] R.C. Gonzalez and R.E. Woods: *Digital Image Processing*, Addison Wesley, New York, 1992.